Metrics of Growth Habit Derived from the 3D Tree Point Cloud Used for Species Determination—A New Approach in Botanical Taxonomy Tested on Dragon Tree Group Example

Petr Vahalík [1],*, Karel Drápela [1], Andrea Procházková [1], Zdeněk Patočka [1], Marie Balková [2], Martin Šenfeldr [3], Klára Lengálová [3], Hana Kalivodová [3], Lucie Vaníčková [3], Lenka Ehrenbergerová [3], Samuel Lvončík [3] and Petr Maděra [3]

[1] Department of Forest Management and Applied Geoinformatics, Faculty of Forestry and Wood Technology, Mendel University in Brno, Zemědělská 1, 613 00 Brno, Czech Republic; karel.drapela@mendelu.cz (K.D.); xprocha4@node.mendelu.cz (A.P.); zdenek.patocka@mendelu.cz (Z.P.)

[2] Department of Geology and Pedology, Faculty of Forestry and Wood Technology, Mendel University in Brno, Zemědělská 1, 613 00 Brno, Czech Republic; marie.balkova@mendelu.cz

[3] Department of Forest Botany, Dendrology and Geobiocoenology, Faculty of Forestry and Wood Technology, Mendel University in Brno, Zemědělská 1, 613 00 Brno Czech Republic; martin.senfeldr@mendelu.cz (M.S.); klara.lengalova@mendelu.cz (K.L.); xkalivo1@mendelu.cz (H.K.); lucie.vanickova@mendelu.cz (L.V.); lenka.ehrenbergerova@mendelu.cz (L.E.); samuel.lvoncik@mendelu.cz (S.L.); petr.madera@mendelu.cz (P.M.)

* Correspondence: petr.vahalik@mendelu.cz; Tel.: +420-545-134-023

Abstract: Detailed, three-dimensional modeling of trees is a new approach in botanical taxonomy. Representations of individual trees are a prerequisite for accurate assessments of tree growth and morphological metronomy. This study tests the abilities of 3D modeling of trees to determine the various metrics of growth habit and compare morphological differences. The study included four species of the genus *Dracaena*: *D. draco*, *D. cinnabari*, *D. ombet*, and *D. serrulata*. Forty-nine 3D tree point clouds were created, and their morphological metrics were derived and compared. Our results indicate the possible application of 3D tree point clouds to dendrological taxonomy. Basic metrics of growth habit and coefficients derived from the 3D point clouds developed in the present study enable the statistical evaluation of differences among dragon tree species.

Keywords: *Dracaena*; photogrammetry; 3D tree point cloud; metrics of growth habit; coefficients of growth habit; taxonomy

1. Introduction

Only a few species among the more than 60–100 species of the genus *Dracaena* from the family *Asparagaceae* [1,2], commonly known as dragon trees, reach a tree growth habit. The genus is found in Macaronesia, Arabia, Socotra, Madagascar, Southeastern Asia, Northern Australia, and the Guinea–Congo region in Western Africa, as well as one species (*D. americana*) that occurs in the neotropics [3].

The dragon tree group, as defined by Marrero et al. [4], includes the following arborescent species: *D. cinnabari* Balf.f., *D. draco* L., *D. tamaranae* A. Marrero, R. S. Almeida & M. González-Martín, *D. ombet* ex Kotschy & Peyr., *D. serrulata* Baker, and *D. schizantha* Baker. The Macaronese and African taxon, *D. draco*, consists of three subspecies: wild populations of *D. draco* subsp. *draco*, only known in

Tenerife and Gran Canaria; a distinct taxon *D. draco* subsp. *ajgal* [5], found in southern Morocco, in the Anti-Atlas region; and *D. draco* subsp. *caboverdeana*, an endemic species of the Capo Verde Islands [6]. *Dracaena cinnabari* is endemic to Socotra Island, where it thrives in the northeastern mountain range of Haggier [7,8], mainly in the highlands of Mumi [9]. Arabian species of *D. serrulata* and *D. ombet* occur along the African hills that face the Red Sea, in Jebel Elba in southeastern Egypt, in Mount Erkowit in Sudan, in the steep slopes of the Eritrean mountains, and in the mountains of Djibouti [10–12]. *Dracaena schizantha* grows in the north-facing slopes of Harar in Ethiopia, in the mountains of Djibouti, and in the northern mountains of Somalia, extending to the Ahl Mountains where it almost reaches the Horn of Africa [13,14]. A further species, *D. hanningtoni*, which is restricted to Mozambique, also appears to be related to the dragon tree group [10].

Current knowledge about the *Dracaena* genus allowed us to extend the dragon tree group to include newly described species from geographical territories other than those mentioned by Marrero et al. [4]. *Dracaena jayniana*, newly described by Wilkin et al. [15], is endemic to central and northeastern Thailand. *Dracaena cambodiana* populations occur in the southwest inland mountains and southern coastal areas of Hainan Island, at altitudes from near sea-level to 900 m [16]. The species is also found in Cambodia, Laos, and Thailand [17]. *Dracaena cochinchinensis* grows in the Yunnan and Guangxi provinces in China, in Vietnam, and in Laos [18]. *Dracaena kaweesakii* is native in north, northeast, and central Thailand and adjacent eastern Myanmar [19]. *Dracaena americana* has a wide distribution across southern Mexico (Tabasco, Veracruz, Quintana Roo, Oaxaca, Chiapas), as well as in Belize, Guatemala, Honduras, Costa Rica, and Panama [3].

Sequence analysis does not support Brown's [2] classification for *Dracaena* to separate arborescent from arbustial species. If the arbustial condition is considered to be ancestral within the phylogeny, then arborescence could have arisen independently several times [20]. *Dracaena tamaranae* seems to be closely related to the three species found in the Horn of Africa and Arabia (i.e., *D. ombet*, *D. schizantha*, and *D. serrulata*) [4]. *D. hanningtoni* also seems to be closely related to *D. ombet* [21]. However, the general shape of the inflorescence indicates that this species seems to be closely related to the *D. draco–D. cinnabari* group. Furthermore, Donnell and Smith [22] place *D. americana* into one section of *Draconis*, together with *D. draco* [23].

The three-dimensional canopy structure data can be obtained for large areas, e.g., using airborne laser scanning [24] or aerial photogrammetry [25]. Because of the view from the top, it is not possible to acquire sufficient detail of the tree structure, especially in the case of canopies' high closure. In addition, aerial photogrammetry has no ability to penetrate canopies and obtain information of a canopy's inner structure because a passive sensor is used [26,27]. In forestry applications, terrestrial laser scanning is being used in order to obtain very detailed point clouds [28]. Nevertheless, the higher costs of laser scanners limit their wider application, especially in developing countries. Therefore, several studies have been published to evaluate the quality of point clouds derived from close-range photogrammetry for application in forestry [26]. Photogrammetric point clouds are being derived through the Structure from Motion (SfM) algorithm [29]. Some studies attribute higher or equal accuracy of these clouds in comparison with the laser-derived point clouds [30,31]. Nevertheless, the impossibility of penetration into the canopy remains. There are two basic approaches for point clouds' workflow, namely, (i) the point-based approach [32] and (ii) the voxel-based approach [33].

The descriptions of all of the above-mentioned *Dracaena* species are based on leaves, flowers, and inflorescence morphology [3,4,6,15,21–23,34]. They differ only in detail, and mostly in quantitative signs rather than qualitative. This makes species estimation among this genus difficult. The dragon tree group is well known due to regular growth, sympodial branching, and the umbrella-shaped crown. The growth habit characteristics of trees are usually used in botanical taxonomy only for general species description. Ocular description does not allow species determination based on the metrics of growth habit of trees. The aim of the present work is to test the possibility of using 3D tree modeling to determine various metrics of growth habit and compare the morphological differences among several *Dracaena* species. This research represents the first description of a nondestructive method using 3D tree modeling, which has not been previously reported in literature.

2. Material and Methods

In the period between 2016 and 2019, 3D tree point clouds were created, and the subsequent metrics of growth habit were determined and statistically evaluated. The study contained four *Dracaena* species: *Dracaena cinnabari*, an endemic species of Socotra Island (Yemen); *Dracaena draco*, which occurs on the Canary Islands (Spain); *Dracaena ombet*, which settled on the north part of Ethiopia; and *Dracaena serrulata*, from the Dhofar mountains in Oman. Only adult trees were included in the analytical process. The age of the trees was determined using the estimation of the mean growth speed of one branch segment (BS) as follows: *Dracaena cinnabari*—19 years/BS; *D. serrulata*—12 years/BS, *D. draco*—10 years/BS; *D. ombet*—7 years/BS [35].

3D tree point clouds were created using terrestrial photogrammetry [36]. The set of overlapping photographs was taken around the tree at different distances and vertical angles (about 150–250 photos for one tree point cloud, depending on the size of the tree). A set of photos was captured to obtain all parts of the tree in perspective. Based on the tree's accessibility and the steepness of the surrounding terrain, two methods were tested and used. Method a) created an outer circle of photos to cover the whole tree habitus and an inner circle to capture the structure of the tree crown in detail (see Figure 1). Method b) used a telescopic camera stick to create two circles of photos with similar diameter and different heights and vertical angles (see Figure 2).
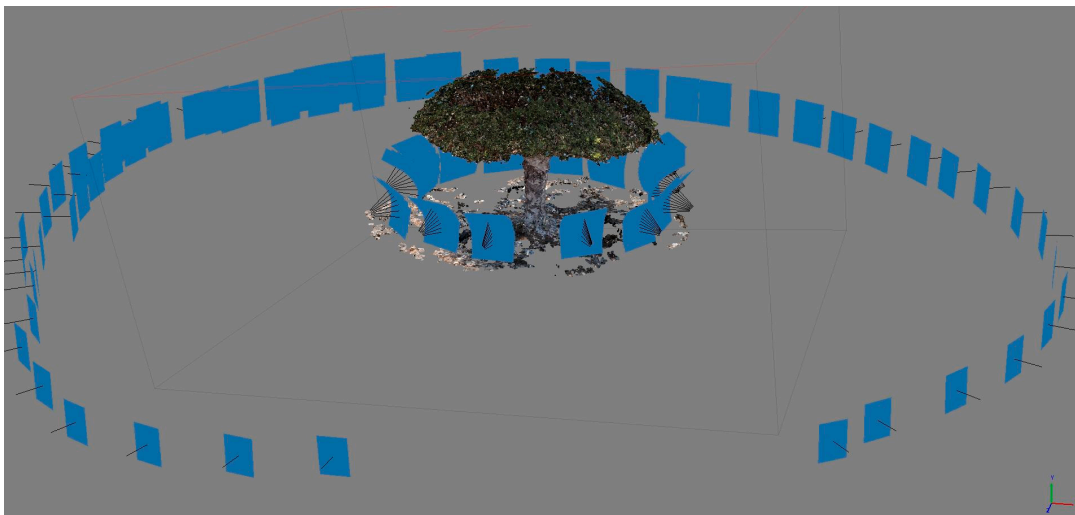
Figure 1. Method a)—position of captured photos to create a photogrammetric 3D tree point cloud. The outer circle of photos captures the whole tree shape. The inner circle of photos consists of the number of photos captured from the same location with various vertical angles to capture the tree structure in detail. Locations are situated all around the tree.

Figure 2. Method b)—position of captured photos to create a photogrammetric 3D tree point cloud. Two circles of photos capture the tree from two vertical angles. The upper circle captures the crown surface, the lower circle captures the stem and the inner structure of the crown.

Photos were processed using Agisoft Metashape software version 1.6.1 (Agisoft LLC, St. Petersburg, Russia). The metrics of the point cloud were defined in a local coordinate network that applies preconfigured prism points with a predefined distance in perpendicular vertical to the Earth's surface (see Figure 3). After the alignment of a sufficient number of pointers in photo overlays, a resulting point cloud was created. On average, the matrix consisted of more than 1.5 million point vectors. Subsequently, the 'noise' was filtered out of the model. The resulting point cloud was exported as a *.las file for further processing.

Figure 3. Prism points with a predefined distance in perpendicular vertical to the Earth's surface. Beads with a mutual distance of 50 cm suspended on a rope ending with the lead are used to define dimensions in the resulting 3D tree point cloud.

Metrics of growth habit were determined using the 3D Forest software version 0.5 (The Silva Tarouca Research Institute for Landscape and Ornamental Gardening–RILOG, Brno, Czech Republic). The first step was a segmentation of the point cloud into individual trees (tree clouds),

which was performed automatically by the previously described algorithm [37]. The following eight metrics were evaluated:

1. Diameter at breast height using randomized hough transformation (DBH–RHT) was calculated as a circle with the center and diameter estimated by the randomized hough transformation algorithm, and with 200 iterations from the tree's DBH subset of the tree point cloud (see Figure 4);

2. Diameter at breast height using the least square's regression (DBH–LSR) was calculated as a circle fitted to the DBH subset of the tree point cloud by the least square's regression. An algebraic estimation of the circle and geometric reduction of squared distances to the computed circle was applied [37];

3. Tree height was computed as a difference of Z coordinates of the highest point of the tree point cloud and tree base position (see Figure 4);

4. Canopy height was computed as a difference of Z coordinates of the highest point of the stem and the highest position of the tree point cloud;

5. Canopy depth was computed as a difference of Z coordinates of the highest point of the stem and the lowest position of the tree point cloud;

6. Convex planar projection of the canopy was based on the convex hull of the tree point cloud orthogonally projected to the horizontal plane (see Figure 4). The convex hull was created by the gift-wrapping algorithm [38];

7. Canopy surface was computed by the triangulation of horizontal canopy sections. The triangulation was based on polygons created by the concave hull of each section (border points). The top and bottom of the crown were triangulated by creating triangles between the highest/lowest point of the crown and the highest/lowest polygon edges, respectively. The rest of the canopy was triangulated by strip triangulation of two consecutive polygons [37];

8. Total tree volume, stem volume, and canopy volume calculations were based on the segmentation of the tree point cloud. Space occupation was calculated for all of the tree segments (see Figure 4). The position of stem centers and stem diameters were calculated at different heights above the tree base position, starting at 0.65 m and followed by 1.3, 2 m, and then every next meter above terrain (see yellow cylinders in Figure 4). The circles (defining the local stem center and diameter) were fitted by the RHT algorithm to horizontal 7 cm slices of the tree point cloud and were clipped at appropriate heights. The algorithm stopped when the estimated diameter reached two times greater value than in both of the two previous circles, which indicated the expansion of the tree cloud into the crown [37].
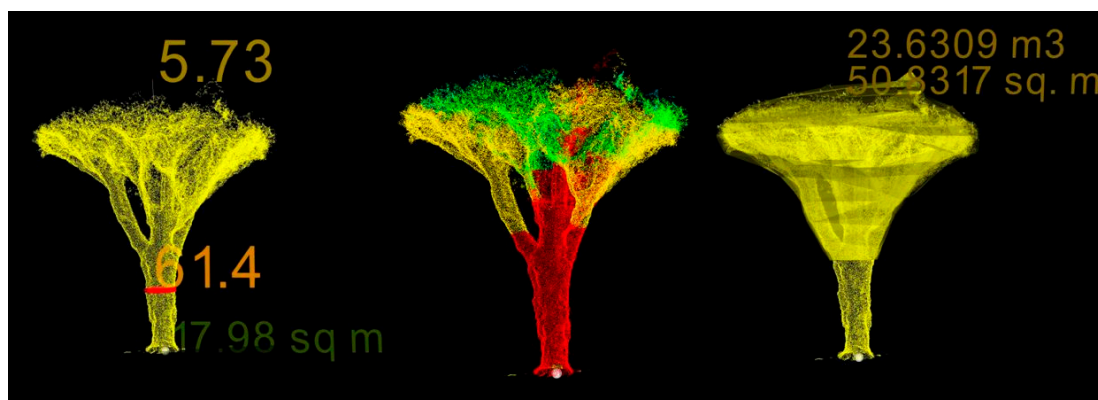
Figure 4. Tree metrics derivation in 3D Forest software. Left: *D. draco* example. Diameter at breast height (DBH), height, and convex planar projection; middle: segmentation of tree in the process of volume calculation; right: canopy volume and surface calculation.

All derived tree metrics were statistically evaluated using Statistica software version 13 (TIBCO Software Inc., Palo Alto, CA, USA). The relationship between age and selected metrics was modeled using linear regression. In addition, several nonlinear models were tested; nevertheless, any

significant improvement in the quality of the model was found. Mean value differences of metrics among individual species were analyzed using one factor analysis of variance (ANOVA). Tukey's test was used as a multiple comparisons test. Comparison of confidence intervals of the metric's mean values is presented in Figure S1. All tests were performed on the significance level $\alpha = 0.05$.

Coefficients of growth habit were determined using a combination of metrics of growth habit. The following coefficients were statistically evaluated:

1. Canopy volume coefficient (CVC) was computed as the ratio of canopy planar projection to canopy volume (CPP/CV);

2. Canopy height coefficient (CHC) was computed as the ratio of canopy depth to canopy height (CD/CH);

3. Stem volume coefficient (SVC) was computed as the ratio of stem volume to total volume (SV/TV);

4. Stem diameter coefficient (SDC) was computed as the ratio of diameter at breast height to canopy depth (DBH/CD).

3. Results

In total, eighty-one individual trees were recorded in Oman, Socotra (Yemen), the northern part of Ethiopia, and on Tenerife Island (Spain). Sets of overlapping photos were captured to create 3D tree point clouds. The success of 3D model creation was based on many parameters, such as light conditions, the position of the sun, accessibility of trees, wind intensity, technical capabilities of the field researcher, and many others. Forty-nine trees were correctly modeled and subsequently analyzed (see Table 1). At least 10 or more point clouds were created for every studied species, except for *D. ombet* due to the strong wind and limited time available for data capturing. Only three models of *D. ombet* were included in the analytical process; thus, the results are not considered statistically significant and are not described in the final results.

**Table 1.** *Dracaena* trees' 3D tree point clouds correctly created.

Species	Number of Recorded Trees	Correctly Created Point Clouds
D. serrulata	25	18
D. cinnabari	30	17
D. draco	16	11
D. ombet	10	3

All metrics of growth habit are depicted in Supplement Table S1. Comparison of specific metrics of growth habit is described in Supplement Figure S1.

Dracaena draco is the tallest and has the thickest stem diameter and stem volume in contrast to *D. serrulata*, which is the shortest and has the smallest stem dimensions. *Dracaena cinnabari* has a larger stem volume compared to smaller DBH due to the high position of canopy depth, which is the highest of all studied species. In the case of *D. draco,* canopy height is the highest of all the species studied. *Dracaena serrulata* has the smallest canopy dimensions (see Figure S1a–c). Values of convex planar projection and canopy surface have a similar course in comparison, as well as values of total volume, and volume of parts thicker than 7 cm, where *D. draco* has the largest dimensions and *D. serrulata* the smallest dimensions (see Figure S1c,d).

There are significant differences in the speed of growth described by DBH and the height of trees compared to their age. Stem diameter of *D. draco* grows at a much faster rate, and individual trees are two times taller than other species of the same age. The growth of DBH and the height of *D. serrulata* show an upward tendency compared to those of *D. cinnabari* (see Figure 5).
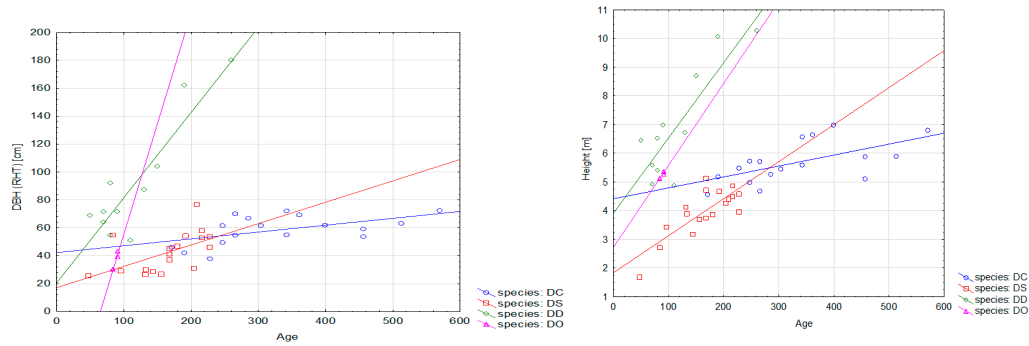
Figure 5. Speed of growth described by DBH and tree height compared to the age of the trees. *Key: DC—Dracaena cinnabari; DS—D. serrulata; DD—D. draco; DO—D. ombet.*

Additionally, the parameters of convex planar projection and the total volume have multiple higher values in the case of *D. draco* when compared with those of other species. Canopy growth and the total volume of *D. serrulata* show a downward tendency compared to those of *D. cinnabari* (see Figure 6).
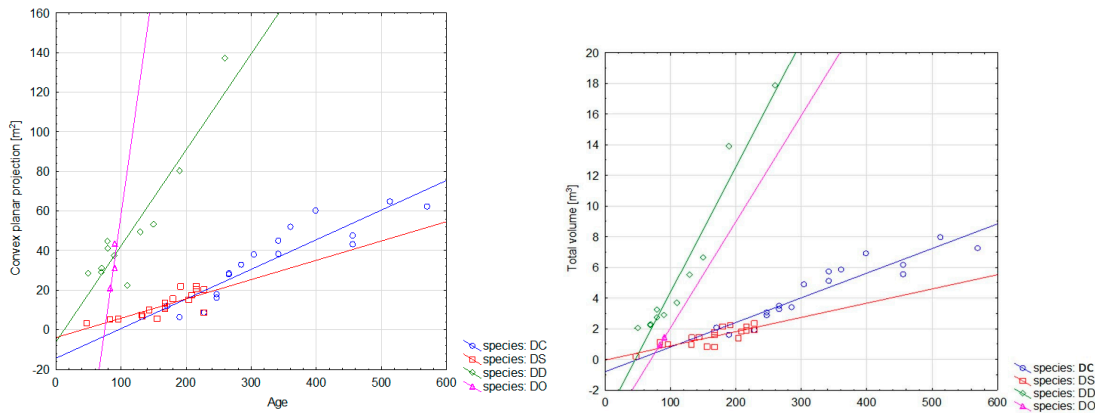

Figure 6. Speed of growth described by convex planar projection and the total volume compared to the age of the trees. *Key: DC—Dracaena cinnabari; DS—D. serrulata; DD—D. draco; DO—D. ombet.*

Dracaena cinnabari has the widest canopy perched on a thinner trunk compared to other species, whereas *D. serrulata* has the smallest canopy growing from a relatively large stem compared to the remaining species (see Figure 7).
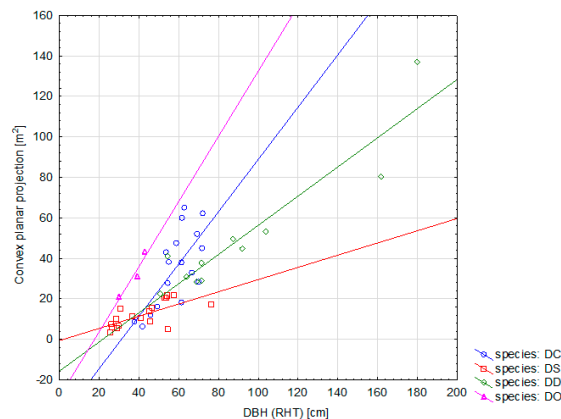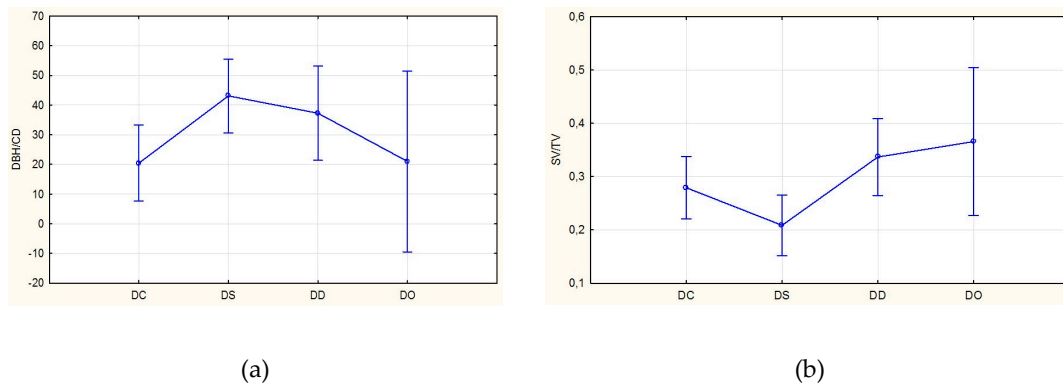

Figure 7. Convex planar projection compared to the stem diameter at breast height (DBH). *Key: DC — Dracaena cinnabari; DS—D. serrulata; DD—D. draco; DO—D. ombet.*

All studied species have similar values of the canopy volume coefficient. *Dracaena draco* has a bigger canopy volume in ratio to convex planar projection. *Dracaena cinnabari* has the shortest canopy with the highest canopy depth compared to other evaluated species (see Figure 8a,b).

(a)   (b)
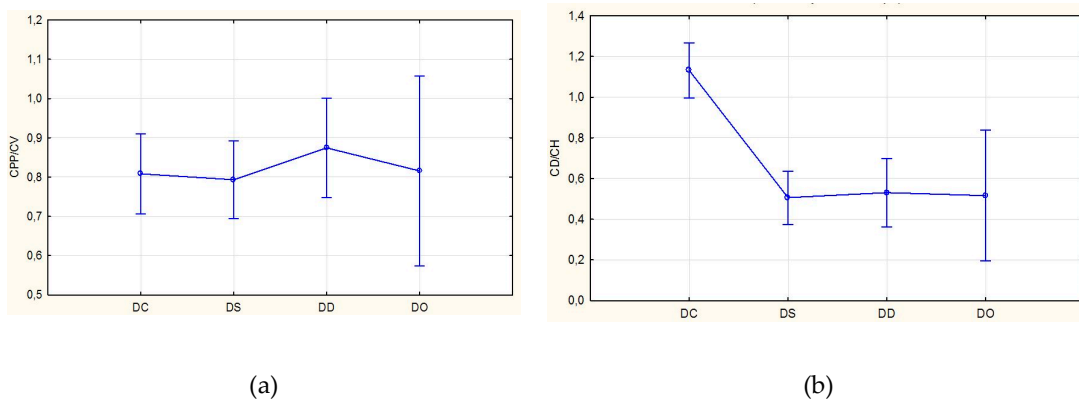
Figure 8. (a) Canopy volume coefficient (CVC) computed as the ratio of canopy planar projection to canopy volume (CPP/CV). (**b**) Canopy height coefficient (CHC) computed as the ratio of canopy depth to canopy height (CD/CH). *Key: DC—Dracaena cinnabari; DS—D. serrulata; DD—D. draco; DO—D. ombet.*

Dracaena draco has a more massive stem compared to the total volume, and *D. serrulata* has the smallest stem in relation to the total volume. *Dracaena cinnabari* has the thinnest and highest stem compared to other studied species (see Figure 9a,b).


(a)   (b)

Figure 9. (a) Stem volume coefficient (SVC) computed as the ratio of stem volume to total volume (SV/TV). (**b**) Stem diameter coefficient (SDC) computed as the ratio of diameter at breast height to canopy depth (DBH/CD). *Key: DC—Dracaena cinnabari; DS—D. serrulata; DD—D. draco; DO—D. ombet.*

The described methodology allows for a visual comparison of the size of the studied *Dracaena* species using the same scale. This approach is unique in comparison with the previously reported methods. Figures 10 and 11 depict the size of the biggest examples of the 3D point clouds created of all studied species in the vertical and horizontal view.
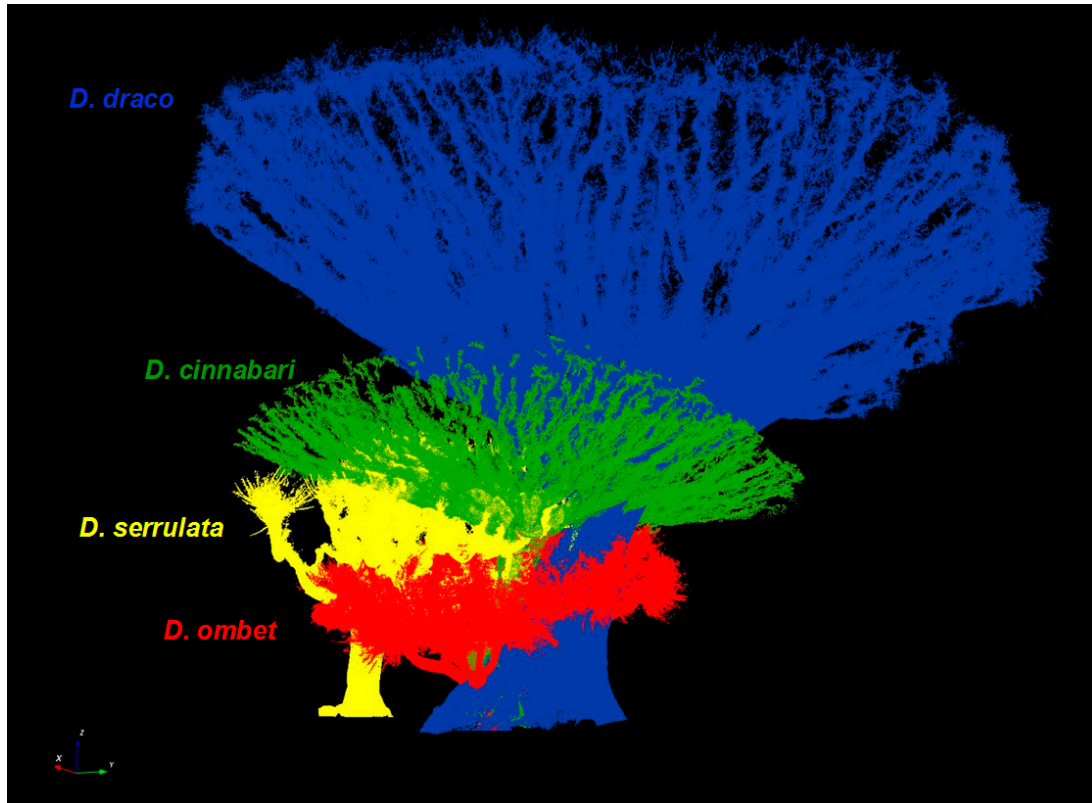
Figure 10. Comparison of the largest examples of created 3D tree point clouds of all studied species in the vertical view depicted with the same scale.
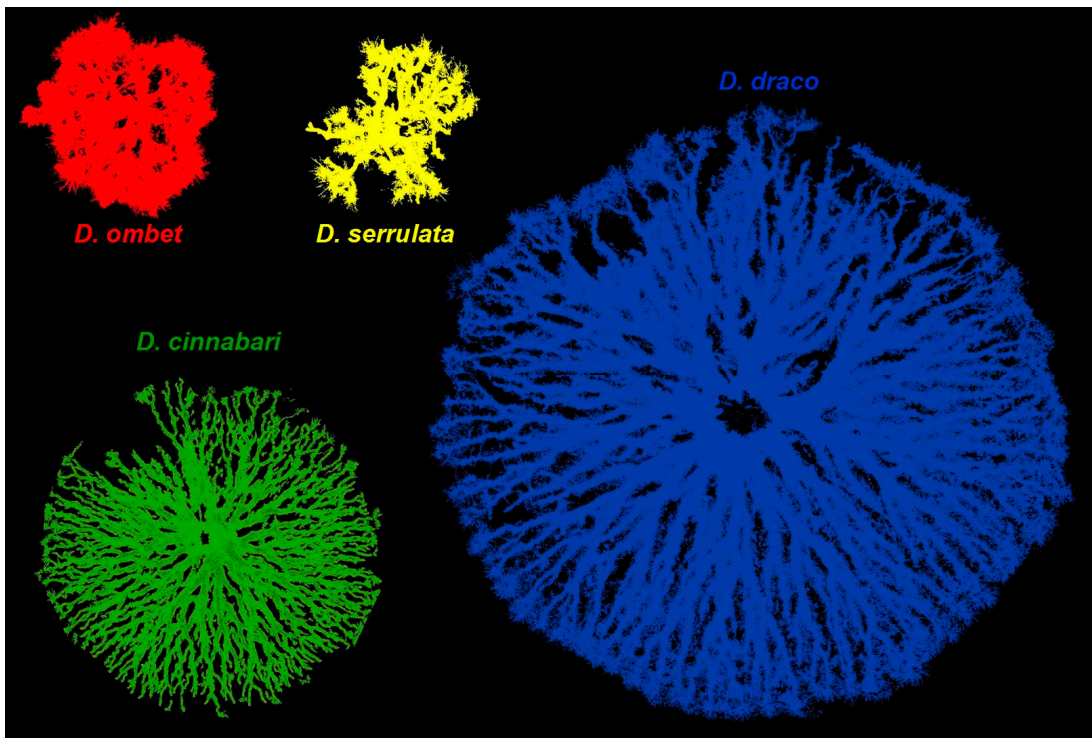
Figure 11. Horizontal cuts of the widest canopy parts of the largest examples of created 3D tree point clouds of all studied species.

4. Discussion

In dendrology, the proper description of tree shape is very complicated [39]; nevertheless, three-dimensional modeling using different techniques can be the solution. Currently, tree models have a wide range of applications. Urban landscape design, ecological simulation, forest management, and virtual entertainment are fields using 3D tree point clouds for different purposes [40]. Some applications (e.g., landscape design and visualization) only require modeling of virtual trees. Many other applications (e.g., ecological modeling and forestry management) require accurate estimation of tree parameters [40]. Similarly, Tu et al. [41] mention the need for accurate 3D models in horticulture.

The tree characteristics usually derived from the 3D tree point clouds are tree height, stem height, DBH, stem basal area, crown projection, and other, more specific parameters such as form factor, leaf area index, stem volume, or crown volume. Manohar and Bharat [42] used mobile laser scanning and a three-dimensional modeling approach for the detection of trees along roads. Qinan Lin et al. [43] detected a pine tree's health status using the 3D tree model created employing a combination of light detection and ranging (LiDAR) and hyperspectral imaging. Mobile laser scanning has wide application in forest inventory [44]. Stationary laser scanning to produce high-precision 3D point clouds is particularly useful for tree stem modeling [45]. In forestry, air/space-borne laser scanning and digital aerial photogrammetry are often used for stock volume estimation [25,46]. Furthermore, different LiDAR scanning techniques are applied to develop the methods of tree leaf area estimation [20,47]. All mentioned characteristics are used more in forestry studies focused on ecology, forest structure, or forest management than in taxonomic studies.

Structure from motion (SfM) photogrammetry has been studied at the plot level in the past few years [48,49]. More studies were focused on measurements of tree position and consequently DBH, height, or stem curve estimation. At the plot level, the root mean square error (RMSE) of DBH, as the most estimated forest variable, ranged from 0.88 to 6.80 cm [26,50,51]. Tree detection ranged between 60% and 98%. At the single tree level, subcentimeter accuracy of DBH estimation was achieved in all studies [52,53]. Bauwens et al. [36] used terrestrial photogrammetry for biomass predictor estimation of buttressed trees in tropical forests. Based on this study, basal area at 1.3 m might be estimated with RMSE less than 5%. As with UAVs (unmanned aerial vehicles), terrestrial photogrammetry does not fully penetrate the canopy [54]. Therefore, SfM point clouds are spatially incomplete as LiDAR point clouds [55]. This can result in poor modeling of branches and leaves inside the crown, or on the canopy top.

In taxonomy, the currently used tree-shape description of different species is mostly based only on the maximum height of the tree and maximum DBH. Using exact metrics of growth habit and different coefficients derived from 3D point clouds could bring new direction into dendrology. Using the method described here allows for description of differences among similar species, as we have shown using the example of dragon trees.

Furthermore, this method describes precisely the different developmental stages of tree ontogeny, which is highly requested in horticulture practice. 3D tree modeling as a nondestructive method allows the comparison of tree growth rates in different environmental conditions, or those under stress applying investigation to the growth of the same tree individuals during a period of time.

The methodology used for the creation of the 3D tree point clouds (photogrammetry) is very sensitive to the environment and the light conditions. The success of this method is also very limited by wind (as demonstrated here in the case of *D. ombet*). A telescopic stick can be replaced by UAV technology to get better results and make the process easier. Other methods of terrestrial scanning, such as terrestrial LiDAR, can be used to enhance the success of 3D model creation. All mentioned technologies can enhance the accuracy and precision of the outputs in the process of 3D modeling in dendrological taxonomy.

5. Conclusions

Our present work describes the possibility of using 3D tree point clouds in dendrological taxonomy. We developed the basic coefficients of growth habit, which were derived from the 3D point clouds metrics, allowing for the statistical evaluation of differences among dragon tree species. The following metrics were proven as useful in dragon tree species differentiation: stem volume, canopy volume, total volume, canopy surface, canopy height, and canopy convex planar projection. All mentioned metrics can be accurately derived from 3D tree point clouds. Coefficients expressed as a ratio of two metrics are also significant in species differentiation. Only four coefficients describing statistically significant differences among species were tested. The methodology used offers development of many other coefficients. Generally, more metrics and consequently more coefficients can be derived and tested, which would enable better possibilities for describing growth differences among species.

Supplementary Materials: The following are available online at www.mdpi.com/xxx/s1, Table S1: Metrics of growth habit of all modeled trees; Figure S1: Comparison of metrics of growth habit.

Author Contributions: Study design, fieldwork, data analysis, and writing the article: P.V. and P.M.; data analysis and writing the article: K.D., S.L., L.V., and M.Š.; data analysis and field work: Z.P., A.P., M.B., L.E., K.L., and H.K. All authors have read and agreed to the published version of the manuscript.

Conflicts of Interest: The authors declare no conflict of interest.

References

1. Mabberley, D.J. *The Plant-Book: A Portable Dictionary of the Higher Plants*; Cambridge Press: Cambridge, UK, 1990.
2. Brown, N.E. Notes on the genera *Cordyline*, *Dracaena*, *Pleomele*, *Sansevieria*, and *Taetsia*. *Bull. Misc. Inf.* (*R. Bot. Gard. Kew*) **1914**, *8*, 273–279.
3. Zona, S.; Álvarez De Zayas, A.; Orellana, R.; Oviedo, R.; Jestrow, B.; Francisco-Ortega, J. *Dracaena* L. (Asparagaceae) in the New World: Its history and Botany. *Vieraea* **2014**, *42*, 219–240.
4. Marrero, A.; Almeida, S.R.; Martín-González, M. A new species of the wild Dragon Tree, *Dracaena* (Dracaenaceae) from Gran Canaria and its taxonomic and biogeographic implications. *Bot. J. Linn. Soc.* **1998**, *128*, 291–314.
5. Benabid, A.; Cuzin, F. Populations de dragonnier (*Dracaena draco* L. subsp. *Aigal* benabid et Cuzin) au Maroc: Valeurs taxinomique, biogéographique et phytosociologique. *C. R. Acad. Sci. Sci. Vie* **1997**, *320*, 267–277.
6. Marrero, A.; Almeida, S.R. A new subspecies, *Dracaena draco* (L.) L. subsp. *Caboverdeana* Marrero Rodr. & R. Almeida (Dracaenaceae) from Cape Verde Island. *Int. J. Geobot. Res*. **2012**, *2*, 35–40. doi:10.5616/ijgr120004.
7. Balfour, B. The dragon's blood tree of Socotra (*Dracaena cinnabari* Balf. fil.). *Trans. R. Soc. Edinb.* **1883**, *30*, 619–623.
8. Maděra, P.; Volařík, D.; Patočka, Z.; Kalivodová, H.; Divín, J.; Rejžek, M.; Vybíral, J.; Lvončík, S.; Jeník, D.; Hanáček, P.; et al. Sustainable land use management needed to conserve the dragon's blood tree of Socotra Island, a vulnerable endemic umbrella species. *Sustainability* **2019**, *11*, 3557; doi:10.3390/su11133557.
9. Beyhl, F.E. Der Drachenbaum und seine Verwandtschaft: II. Der echte Drachenbaum, *Dracaena cinnabari*, von der Insel Sokotra. *Palmengarten* **1995**, *59*, 140–145.
10. Baker, J.G. Liliaceae: *Dracaena*. In *Flora of Tropical Africa*, *Hydrocharideae to Liliaceae*; Thiselton-Dyer, W.T., Ed.; L. Reeve & Co.: Ashford, UK, 1898; Volume 2, pp. 436–450.
11. Täckholm, V.; Drar, M. *Flora of Egypt. Volume III*: *Angiospermae, Part Monocotyledones*: *Liliaceae-Musaceae*, 2nd ed.; Otto Koeltz Antiquariat: Koenigstein, Germany, 1973.
12. Friis, I. *Forests and Forest Trees of Northeast Tropical Africa*; New Bulletin Addition Series XV; Her Majesty's Stationery Office (HMSO): Richmond, UK; Royal Botanic Gardens, Kew: Richmond, UK, 1992.

13. Baker, J.G. *Dracaena schizantha*. In *the Journal of Botany*, *New Series*; Trimen, H., Ed.; Ranken & Co: London, UK, 1877; Volume 6, p. 71.

14. Thulin, M. Dracaenaceae. In *Flora of Somalia*; Thulin, M., Ed.; Royal Botanic Gardens, Kew: Richmond, UK, 1995; Volume 4, pp. 27–30.

15. Wilkin, P.; Suksathan, P.; Keeratikiat, K.; Van Welzen, P.; Wiland-Szymanska, J. A new threatened endemic species from central and northeastern Thailand, *Dracaena jayniana* (Asparagaceae: Tribe Nolinoideae). *Kew Bull*. **2012**, *67*, 697–705.

16. Zheng, D.J.; Xie, L.S.; Zhu, J.H.; Zhang, Z.L. Low genetic diversity and local adaptive divergence of *Dracaena cambodiana* (Liliaceae) populations associated with historical population bottlenecks and natural selection: An endangered long-lived tree endemic to Hainan Island, China. *Plant Biol*. **2012**, *14*, 828–838, doi:10.1111/j.1438-8677.2011.00559.x.

17. Chen, X.Q.; Turland, N.J. *Dracaena vandelli* ex *Linnaeus*. In *Flora of China*; Wu, Z.Y., Raven, P.H., Eds.; Science Press: Beijing, China; Missouri Botanical Garden Press: St. Louis, MO, USA, 2000; Volume 24, pp. 215–217,

18. Fan, J.Y.; Yi, T.; Sze-To, C.M.; Zhu, L.; Peng, W.L.; Zhang, Y.Z.; Zhao, Z.Z.; Chen, H.B. A Systematic review of the botanical, phytochemical and pharmacological profile of *Dracaena cochinchinensis*, a plant source of the ethnomedicine "Dragon's Blood". *Molecules* **2014**, *19*, 10650–10669, doi:10.3390/molecules190710650.

19. Wilkin, P.; Suksathan, P.; Keeratikiat, K.; Van Welzen, P.; Wiland-Szymanska, J. A new species from Thailand and Burma, *Dracaena kaweesakii* Wilkin & Suksathan (Asparagaceae subfamily Nolinoideae). *PhytoKeys* **2013**, *26*, 101–112, doi:10.3897/phytokeys.26.5335.

20. Lu, P.-L.; Morden, C.W. Phylogenetic relationships among *Dracaenoid genera* (Asparagaceae: Nolinoideae) inferred from Chloroplast DNA Loci. *Syst. Bot.* **2014**, *39*, 90–104, doi:10.1600/036364414X678035.

21. Baker, J.G. *Dracaena ombet* Kotschy et Peir. In *Hooker's Icones Plantarum*; Ser. 4, Part II; Thiselton-Dyer, W.T., Ed.; Dulay & Co.: London, UK, 1897; Volume 6, plate 2539.

22. Donnell Smith, J. *Dracaena americana*. In *Trees and Shrubs. Illustrations of New or Little Known Ligneous Plants*; Sargent, C.S., Ed.; Houghton, Mifflin and Company: Boston, MA, USA; New York, NY, USA, 1905; Volume 1, p. 207.

23. Baker, J.G. Revision of the genera and species of Asparagaceae. *J. Lin. Soc. Bot*. **1875**, *14*, 508–632.

24. Hyyppä, J.; Hyyppä, H.; Leckie, D.; Gougeon, F.; Yu, X.; Maltamo, M. Review of methods of small-footprint airborne laser scanning for extracting forest inventory data in boreal forests. *Int. J. Remote Sens*. **2008**, *29*, 1339–1366.

25. Puliti, S.; Hauglin, M.; Breidenbach, J.; Montesano, P.; Neigh, C.S.R.; Rahlf, J.; Solberg, S.; Klingenberg, T.F.; Astrup, R. Modelling above-ground biomass stock over Norway using national forest inventory data with ArcticDEM and Sentinel-2 data. *Remote Sens. Environ*. **2020**, *236*, 111501, doi:10.1016/j.rse.2019.111501.

26. Mikita, T.; Janata, P.; Surový, P. Forest stand inventory based on combined aerial and terrestrial close-range photogrammetry. *Forests* **2016**, *7*, 165.

27. Wallace, L.; Lucieer, A.; Malenovský, Z.; Darren, T.; Vopěnka, P. Assessment of forest structure using two UAV techniques: A comparison of airborne laser scanning and structure from motion (SfM) point clouds. *Forests* **2016**, *7*, 62.

28. Dassot, M.; Constant, T.; Fournier, M. The use of terrestrial LiDAR technology in forest science: Application fields, benefits and challenges. *Ann. For. Sci*. **2011**, *68*, 959–974.

29. Lowe, D.G. Method and Apparatus for Identifying Scale Invariant Features in an Image and Use of Same for Locating an Object in an Image. U.S. Patent 6,711,293, 23 March 2004.

30. Kangas, A.; Gobakken, T.; Puliti, S.; Hauglin, M.; Næsset, E. Value of airborne laser scanning and digital aerial photogrammetry data in forest decision making. *Silva Fenn.* **2018**, *52*, 19, doi:10.14214/sf.9923.

31. Hrůza, P.; Mikita, T.; Tyagur, N.; Krejza, Z.; Cibulka, M.; Procházková, A.; Patočka, Z. Detecting forest road wearing course damage using different methods of remote sensing. *Remote Sens.* **2018**, *10*, 492.

32. Li, Y.; Guo, Q.; Su, Y.; Tao, S.; Zhao, K.; Xu, G. Retrieving the gap fraction, element clumping index, and leaf area index of individual trees using single-scan data from a terrestrial laser scanner. *ISPRS J. Photogramm. Remote Sens*. **2017**, *130*, 308–316.

33. Hosoi, F.; Omasa, K. Voxel-Based 3-D modeling of individual trees for estimating leaf area density using high-resolution portable scanning Lidar. *IEEE Trans. Geosci. Remote Sens*. **2006**, *44*, 3610–3618.

34. Hubálková; I; Maděra, P.; Volařík, D. Growth dynamics of *Dracaena cinnabari* under controlled conditions as the most effective way to protect endangered species. *Saudi J. Biol. Sci*. **2017**, *24*, 1445–1452, doi:10.1016/j.sjbs.2015.09.011.

35. Adolt, R.; Habrová; H; Maděra, P. Crown age estimation of a monocotyledonous tree species *Dracaena cinnabari* using logistic regression. *Trees Struct. Funct.* **2012**, *26*, 1287–1298, doi:10.1007/s00468-012-0704-9.

36. Bauwens, S.; Fayolle, A.; Fleury, S.; Ndjele, L.; Mengal, C.; Lejeune, P. Terrestrial photogrammetry: A non-destructive method for modelling irregularly shaped tropical tree trunks. *Methods Ecol. Evol.* **2017**, doi:10.1111/2041-210X.12670.

37. Trochta, J.; Krůček, M.; Vrška, T.; Král, K. 3D Forest: An application for descriptions of three-dimensional forest structures using terrestrial LiDAR. *PLoS ONE* **2017**, *12*, e0176871.

38. Preparata, F.P.; Hong, S.J. Convex hulls of finite sets of points in two and three dimensions. *Commun. ACM* **1977**, *20*, 87–93.

39. Maděra, P.; Slach, T.; Úradníček, L.; Lacina, J.; Černušáková, L; Friedl, M.; Řepka, R. Tree shape and form in ancient coppice woodlands. *J. Landsc. Ecol.* **2017**, *10*, 5–18, doi:10.1515jlecol-2017-0004.

40. Du, S.; Lindenbergh, R.; Ledoux, H.; Stoter, J.; Nan, J. AdTree: Accurate, detailed, and automatic Modelling of laser-scanned trees. *Remote Sens.* **2019**, *11*, 2074, doi:10.3390/rs11182074.

41. Tu, Y.H.; Phinn, S.; Johansen, K.; Robson, A.; Wu, D. Optimising drone flight planning for measuring horticultural tree crop structure. *ISPRS J. Photogramm. Remote Sens*. **2020**, *160*, 83–96, doi:10.1016/j.isprsjprs.2019.12.006.

42. Manohar, Y.; Bharat, L. Identification of trees and their trunks from mobile laser scanning data of roadway scenes. *Int. J. Remote Sens.* **2020**, *41*, 1233–1258, doi:10.1080/01431161.2019.1662966.

43. Qinan, L.; Huaguo, H.; Jingxu, W.; Kan, H.; Yangyang, L. Detection of pine shoot beetle (PSB) stress on pine forests at individual tree level using UAV-based hyperspectral imagery and lidar. *Remote Sens.* **2019**, *11*, 2540, doi:10.3390/rs11212540.

44. Holmgren, J.; Tulldahl, M.; Nordlöf, J.; Willén, E.; Olsson, H. Mobile laser scanning for estimating tree stem diameter using segmentation and tree spine calibration. *Remote Sens.* **2019**, *11*, 2781, doi:10.3390/rs11232781.

45. Thies, M.; Pfeifer, N.; Winterhalder, D.; Gorte, B.G.H. Three-Dimensional reconstruction of stems for assessment of taper, sweep and lean based on laser scanning of standing trees. *Scand. J. For. Res.* **2004**, *19*, 571–581, doi:10.1080/02827580410019562.

46. Guerra-Hernández, J.; Cosenza, D.N.; Cardil, A.; Silva, C.A.; Botequim, B.; Soares, P.; Silva, M.; González-Ferreiro, E.; Díaz-Varela, R.A. Predicting Growing stock volume of eucalyptus plantations using 3-D point clouds derived from UAV imagery and ALS data. *Forests* **2019**, *10*, 905, doi:10.3390/f10100905.

47. Yun, T.; Cao, L.; An, F.; Chen, B.; Xue, L.; Li, W.; Pincebourde, S.; Smith, M.J.; Eichhorn, M.P. Simulation of multi-platform LiDAR for assessing total leaf area in tree crowns. *Agric. For. Meteorol*. **2019**, *276–277*, 107610, doi:10.1016/j.agrformet.2019.06.009.

48. Meesuk, V.; Vojinovic, Z.; Mynettac, A.; Abdullah, A.F. Urban flood modelling combining top-view LiDAR data with ground-view SfM observations. *Adv. Water Resour*. **2015**, *75*, doi:10.1016/j.advwatres.2014.11.008.

49. Gergeľová, M.; Kuzevičová, Ž.; Labant, S.; Gašinec, J.; Kuzevič, Š.; Unucka, J.; Liptai, P. Evaluation of selected sub-elements of spatial data quality on 3D flood event modeling: Case study of Prešov City, Slovakia. *Appl. Sci.* **2020**, *10*, doi:10.3390/app10030820.

50. Mokroš, M.; Liang, X.; Surový, P.; Valent, P.; Čerňava, J.; Chudý. Evaluation of close-range photogrammetry image collection methods for estimating tree diameters. *Int. J. Geo Inf.* **2018**, *7*, 93.

51. Piermattei, L.; Karel, W.; Wang, D.; Wieser, M.; Mokroš, M.; Surový, P.; Koreň, M.; Tomaštík, J.; Pfeifer, N.; Hollaus, M. Terrestrial structure from motion photogrammetry for deriving forest inventory data. *Remote Sens.* **2019**, *11*, 950.

52. Mokroš, M.; Výbošťok, J.; Tomaštík, J.; Grznárová, A.; Valent, P.; Slavík, M.; Merganič, J. High precision individual tree diameter and perimeter estimation from close-range photogrammetry. *Forests* **2018**, *9*, doi:10.3390/f9110696.

53. Surový, P.; Yoshimoto, A.; Panagiotidis, D. Accuracy of reconstruction of the tree stem surface using terrestrial close-range photogrammetry. *Remote Sens*. **2016**, *8*, 1–13.

54. Dandois, J.P.; Ellis, E.C. Remote sensing of vegetation structure using computer vision. *Remote Sens.* **2010**, *2*, 1157–1176.

55. Mlambo, R.; Woodhouse, I.H.; Gerard, F.; Anderson, K. Structure from motion (SfM) photogrammetry with drone data: A low cost method for monitoring greenhouse gas emissions from forests in developing countries. *Forests* **2017**, *8*, 68.